MATERIALS PHYSICS AND MECHANICS RESEARCH ARTICLE

Submitted: September 19, 2024 **Revised: October 12, 2024** **Accepted: December 9, 2024**

Finite element analysis for prediction of femoral component strength in hip joint endoprosthesis made from meta-biomaterial

A.I. Borovkov [1], L.B. Maslov [1,2], M.A. Zhmaylo [1]✉, F.D. Tarasenko [1], L.S. Nezhinskaya [1]

[1] Peter the Great St. Petersburg Polytechnic University, St. Petersburg, Russia

[2] Ivanovo State Power Engineering University, Ivanovo, Russia

✉ zhmaylo@compmechlab.com

ABSTRACT

A theoretical study on the structural strength of an endoprosthesis stem made from meta-biomaterial is presented. We considered six types of metamaterials based on a biocompatible titanium alloy comprised by unit cells of lattice and surface structures. The standard for testing femoral components of endoprostheses was used to develop virtual test benches for simulation of the loading process, followed by stress–strain analysis of meta-biomaterial implants. Our general findings confirm the load-bearing capacity of the structures, additionally pointing to potential issues that may arise if the manufacturing technology of metamaterial endoprostheses is insufficiently rigorous.

KEYWORDS

meta-biomaterial • lattice structures • surface structures • hip joint • endoprosthesis • finite element analysis • strength

Acknowledgements. *This work has been supported by the grants the Russian Science Foundation, RSF 23-19-00882.*

Citation: Borovkov AI, Maslov LB, Zhmaylo MA, Tarasenko FD, Nezhinskaya LS. Finite element analysis for prediction of femoral component strength in hip joint endoprosthesis made from meta-biomaterial. *Materials Physics and Mechanics*. 2024;52(6): 38–60.
http://dx.doi.org/10.18149/MPM.5262024_5

Introduction

Metamaterials are understood as artificial macroscale structures composed from periodically repeated highly porous structural elements of the smallest size (micro-, meso-, nano-scale). The term 'metamaterials' reflects the fact that the complex internal structure of such materials at the mesoscale induces peculiar physical and mechanical properties at the macroscale, not observed in natural materials and alloys obtained by conventional methods or in other synthetic substances. A new approach, drawing on the physical principles and computational models to engineer materials with unique properties and advanced functionality, has become known as rational design (RD) [1]. The RD approach was first adopted to design the mechanical [2], electromagnetic [3], acoustic [4] and poroelastic [5] properties for modern functional metamaterials in various engineering fields other than biological and clinical medicine.

Specifically, meta-biomaterials [6] have gained attention in regenerative medicine as potential candidates for various medical and clinical applications, including tissue and organ repair. Key applications of meta-biomaterials in tissue engineering are engineering of three-dimensional structures, such as scaffolds, serving as temporary structural support for tissue regeneration, or such as implants and endoprostheses, which are artificial substitutes for individual organs or their parts, installed permanently in the

human body. Meta-biomaterials can be designed to mimic the biomechanical properties of natural tissues. For example, they may exhibit certain elastic stiffness properties, making them better suited to the mechanical requirements for repaired tissues and organs.

Importantly, the understanding of meta-biomaterials within the context of tissue engineering is rather more elaborate than the model of highly porous materials with complex internal structure, made from biocompatible metal or plastic. Meta-biomaterials are assumed to differ significantly from the vast majority of other metamaterials known today in that they are intended for simultaneously providing physical properties of dissimilar nature [6]. In this sense, meta-biomaterials can be regarded as multiphysical metamaterials in contrast to classical metamaterials designed to provide one type of physical properties, such as mechanical, acoustic or optical metamaterials. A crucial range of properties of a different physical nature are biophysical and biomechanical characteristics of living tissues (in particular, bone) that must be reproduced by meta-biomaterials. In addition to purely mechanical properties (elasticity, strength, stiffness), these include mass transport properties and topological characteristics necessary for functional and reparative regeneration of bone tissue [7]. Thus, a high level of porosity and an extensive network of pore channels in bone scaffolds and implants made from meta-biomaterials are the primary mechanobiological factors [8] deciding the efficiency of regenerative processes in the volume of artificial substitutes for human skeletal elements [9,10].

Endoprostheses with a developed porous surface based on biocompatible alloys are widely used in regenerative medicine to repair large bone defects of the human musculoskeletal system. Extensive bone defects resulting from injury, tumor or other pathological conditions require implants that can not only provide mechanical support but also promote restoration of the bone structure by stimulating osteogenesis (growth of new bone tissue), ensuring osseointegration (ingrowth of bone tissue into the pore space of the implant) and vascularization (growth of vessels in the defect site to improve blood supply) [11,12]. However, only the surface layer of limited thickness typically has a porous structure in most standard endoprostheses. Therefore, it is of utmost importance to carry out research into meta-biomaterials to develop new types of endoprostheses with through-porosity for major joints. Meta-biomaterials can help answer these biomedical challenges, thanks to their multiphysical nature.

Another critical problem occurring during deployment of all-metal endoprostheses and the patient's daily activities is the so-called stress shielding effect [13]. Due to high stiffness of the femoral stem in the hip endoprosthesis prepared by the standard procedure from a titanium alloy, stress redistribution occurs within the bone–implant system, since most of the load is taken by the metal structure. This results in a decreased stress level in the cortical bone tissue forming the medullary canal, where the bone is adjacent to the endoprosthesis. According to Wolff's law [14] and the main hypotheses of modern mechanobiology [15], this in turn leads to activation of specific bone cells (osteoclasts) responsible for the destruction of bone tissue, due to reduced stresses in the bone volume in the contact region between the bone and the endoprosthesis. Consequently, the processes of bone resorption are accelerated, becoming more prevalent than the processes of new bone tissue growth. Thus, the density and associated

strength characteristics of bone tissue decrease, leading over time to micro-destruction of bone at the interface with metal, weakening the fixation of the stem in the medullary canal, ultimately resulting in loosening or even complete dislocation.

Efforts to resolve this issue are underway in orthopedics, with alternative approaches adopting softer biocompatible polymers instead of metals [16]. Successful attempts to mitigate the stress-shielding effect include endoprosthesis components made of polyetheretherketone reinforced by carbon fibers (PEEK/CF) [17,18]. However, such approaches typically do not incorporate porous structures based on polymer materials due to a significant decrease in the strength of the implant, especially for highly loaded skeletal sites [19]. Therefore, another promising scenario explored in this study, reducing the integral stiffness of the structure while preserving the necessary strength, consists of using porous metamaterials based on biocompatible alloys with highly tunable effective elastic and strength properties [20,21].

The fundamental dependence of macroscopic properties of metamaterials on the microscale topology has sparked intense research into the characteristics of the internal structure determined by the geometry of the repeated unit cell [22,23]. The first types of meta-biomaterials, that is, metamaterials intended for tissue engineering, were designed based on unit cells that are strut microstructures, ranging from simple cube-like shapes to complex assemblies composed of multiple struts [24]. Unit cells of such beam-like metamaterials mimic the crystal lattices of metals, repeating their spatial symmetry groups [25]. Experimental clinical studies have confirmed that optimized lattice implants can be used in surgical procedures to partially replace the tubular bone with sufficiently long scaffolds [26]0. The proposed technique for developing a special type of metamaterial is based on a unit cell containing a pore of variable elliptical shape and orientation. The technique proved successful for the case of a hip endoprosthesis stem, reducing the weight of the structure by 9–11%, depending on the type of implant, while preserving structural strength [27]. Treatment of bone defects using open-pore scaffolds based on beam elements with strut diameters ranging from 200 to 500 μm is discussed in [28], detailing the structural optimization of a titanium scaffold to match its elastic properties to cortical bone tissue. The paper investigates the mechanical behavior of the constructed models of metamaterials, establishing the dependence of the elastic modulus on the characteristics of beam-type structures.

Metamaterials based on smooth surfaces in 3D space appeared later than structures based on beam elements. They offer an advantage over lattice-type metamaterials in specific applications necessitating a highly developed internal structure formed by a flow-through system of interconnected pore channels with curvature smoothing. A prominent class is metamaterials based on triply periodic minimal surfaces (TPMS) [29]0. TPMS are a family of periodically repeated implicit surfaces with zero mean curvature, i.e., local minimization of the surface area for a three-dimensional domain with a predefined interface. A metamaterial based on triply periodic minimal surfaces consists of infinite non-intersecting shells of a given thickness, repeating in the directions of three coordinate axes with a fixed or varying period. The internal surfaces of TPMS metamaterials have large specific area, making them good candidates for chemical microreactors, membrane devices, fuel elements, energy absorbers (for kinetic, thermal, acoustic wave energy, microwave electromagnetic waves) [29].

Much research is carried out into the biomedical applications of this family of metamaterials as bone scaffolds or implants. The reason for the attention that this topic has received is that effective osseointegration requires for artificial bone substitutes to have an extensive system of open-type pore channels for migration and transformation of active cells into bone matter, simultaneously providing sufficient strength to ensure the functionality of organs, especially the human musculoskeletal system. Metamaterials of this type offer potential advantages over the beam type due to larger area of internal surfaces, whose curvature is close to the curvature of trabecular bone tissue with its extensive system of pore channels. It was recently found that the surface curvature strongly affects tissue regeneration [30], and since the mean surface curvature of the trabecular bone is close to zero, meta-biomaterials based on TPMS should provide more efficient regeneration of biological tissue in the void space of the scaffold [31].

Even though additive technologies are becoming increasingly popular for manufacturing customized implants and endoprostheses, including those with an arbitrary porous [32] or periodic lattice structure [33–35], theoretical predictions of strength are still scarce, generally limited to studies of failure at the mesoscale level of the metamaterial unit cell [36] or using averaged models. A separate challenge is the construction of full-scale high-fidelity finite element models for endoprostheses made from meta-biomaterials and ab initio calculations of the stress–strain state of the endoprostheses, as these models must avoid simplifications and homogenization of elastoplastic properties [37].

Few papers are available for relatively small-sized lattice models of implants [26]0, [27,28] and endoprostheses [38,39], aimed at direct finite element analysis (FEA) of the stress distribution. Moreover, there are virtually no computational studies on the strength predictions for endoprostheses made of complex structural meta-biomaterials (in particular, surface-type) providing raw data without resorting to averaging procedures. The likely reason for this is that direct FEA simulation of the periodic internal spatial structure of lattice and, especially, surface metamaterials is very complex. On the other hand, it is crucial to obtain predictions of strength and fatigue resistance, as endoprostheses of major joints must be able to withstand substantial force during many loading cycles during the patient's normal motor activity after surgery.

This study is focused on designing the femoral stem for a human hip endoprosthesis made from a meta-biomaterial with through-porosity and a complex internal structure, which is one of the practical applications of metamaterials in tissue engineering. We characterized three configurations of meta-biomaterial based on lattice structures and three configurations based on triply periodic minimal surfaces. The main objective of the study is the theoretical evaluation of strength in an endoprosthesis stem, following the standard test procedure for biomedical products based on continuum mechanics.

Materials and Methods

Types of metamaterials

Meta-biomaterials based on Ti_6Al_4V titanium alloy were selected to develop models of candidate structures for the femoral component (stem) of hip endoprosthesis. This alloy is widely used in surgical procedures to replace bone structures with artificial

components due to its high strength properties, chemical stability and biocompatibility. This material can be used to manufacture components with thin elements and complex geometries and is also well-suited for products with requirements for minimal weight.

Three types of rod cells and three types of TPMS-based cells were taken as unit cells composing the metamaterials, while their geometry was tailored so that the bulk porosity and the content of the base material were the same for all types of cells. The overall dimensions of the cells were 3.7 × 3.7 × 3.7 mm^3, the porosity was 70 %, and the content of the base material 30 %.

Lattice metamaterials are represented in this study by the following structures: cubic with supports, diamond, double pyramid. Surface metamaterials were developed based on the following TPMS: Gyroid, Fischer–Koch, Schwarz D (Fig. 1). A detailed description of the procedure for constructing the unit cells of beam and surface-based metamaterials is provided in our previous studies [20,21].

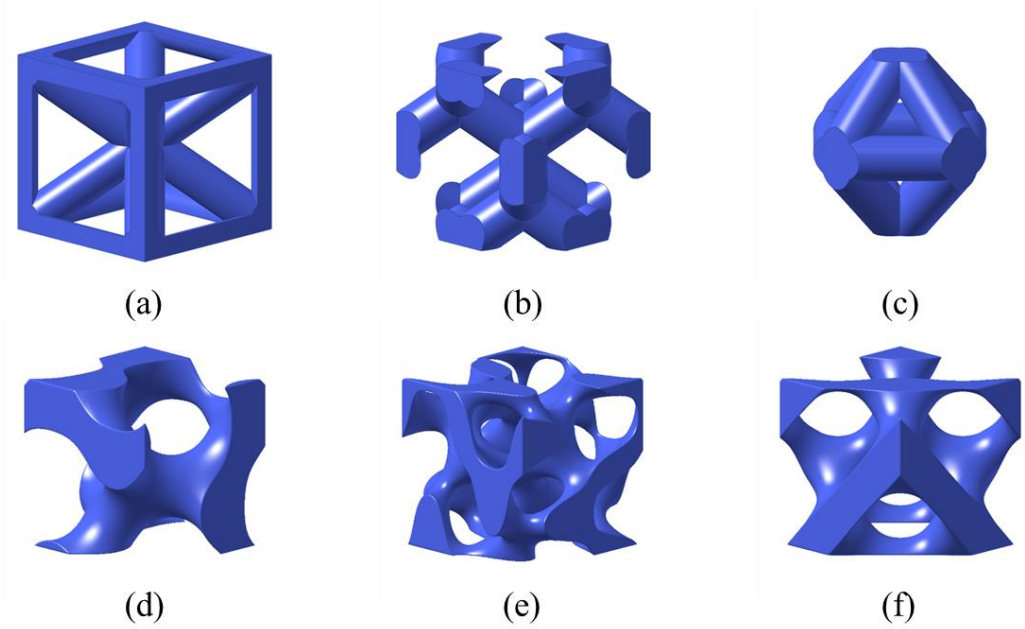

Fig. 1. Unit cells of six types of metamaterials: (a) Cubic with supports; (b) Diamond; (c) Double pyramid; (d) Gyroid; (e) Fischer–Koch; (f) Schwarz D

Model of endoprosthesis stem made from metamaterial

The external shape of the developed structure has a standard topology repeating the curvature of the proximal femur along the force lines, as described in an earlier study [40]. The overall dimensions of the stem were 176 × 66 × 15 mm^3. Figure 2 illustrates the construction of the three-dimensional model for the femoral component of the hip endoprosthesis made from meta-biomaterial. Three-dimensional geometric models of the stem based on lattice metamaterials were built in the ANSYS SpaceClaim module, and the models of the stem based on surface elements were built in the Altair Inspire software. The endoprosthesis stem based on the unit cells considered was developed in the following stages:

1. Construction of a parallelepiped or other shape closer to the target shape, circumscribed around the implant (Fig. 2(a)). This region is filled with metamaterial composed of 3.7 × 3.7 × 3.7 mm^3 cells with a porosity of 70 %.
2. Export of the initial solid implant model from the STEP file format representing geometric data into the STL file format with a triangular surface mesh size of 0.2 mm (Fig. 2(b)).
3. Boolean intersection of the metamaterial preform with the target geometry of the solid implant in mesh format. The resulting implant is made from solid metamaterial without additional elements necessary for the femoral component of the hip endoprosthesis (Fig. 2(c)).
4. Completion of the stem model by replacing a part of the metamaterial in the proximal region of the implant with solid material for attaching the endoprosthesis head (Fig. 2(d)).

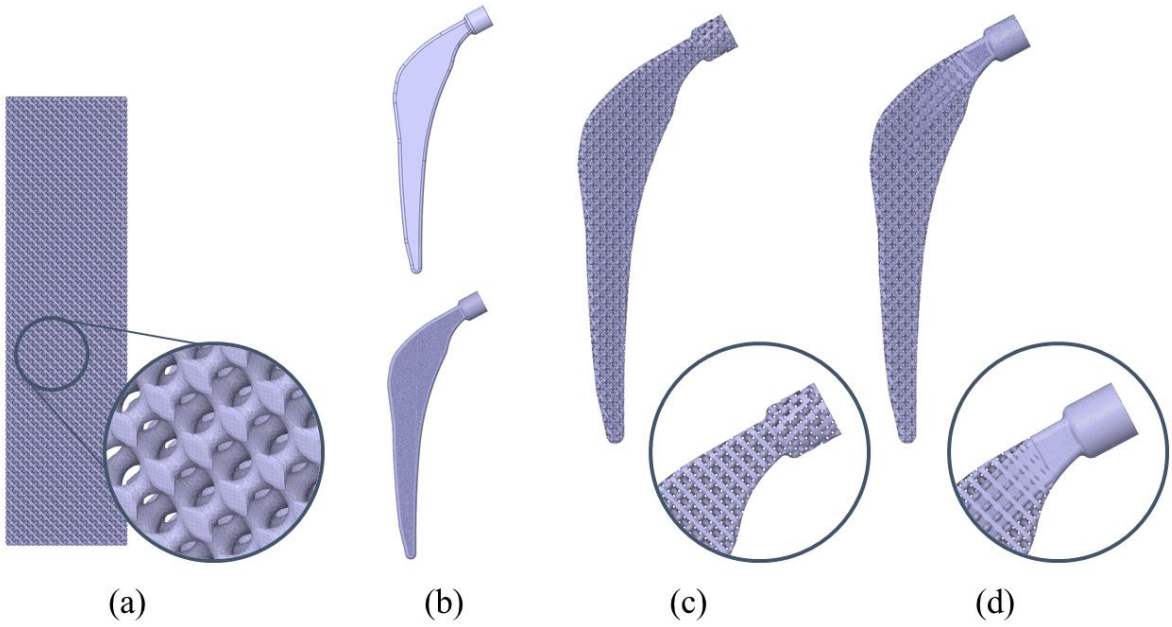

Fig. 2. Construction of model for femoral component of hip endoprosthesis manufactured from typical metamaterial: (a) metamaterial preform; (b) target geometry of stem in STEP and STL formats; (c) intermediate model of stem made entirely from metamaterial; (d) final model of femoral component made from metamaterial with solid head

A three-dimensional model of the structure built was saved in STL format and then exported to the Altair SimLab system for automatic construction of a three-dimensional mesh of tetrahedral finite elements. Because the surface of the implant composed of metamaterial cells has a very complex shape, the finite element mesh contains a large number of thin or self-intersecting elements along the outer edge. These low-quality elements need to be further modified to reliably obtain the stress fields in the structure. Small elements that do not meet the criteria for mesh quality are automatically detected in the Altair SimLab system, and subsequently corrected or deleted. The finite element model adjusted by this technique is again converted to neutral format of STL surface

mesh for subsequent steps. Figure 3 shows three-dimensional geometric models of the endoprosthesis stem made from all six types of metamaterials.

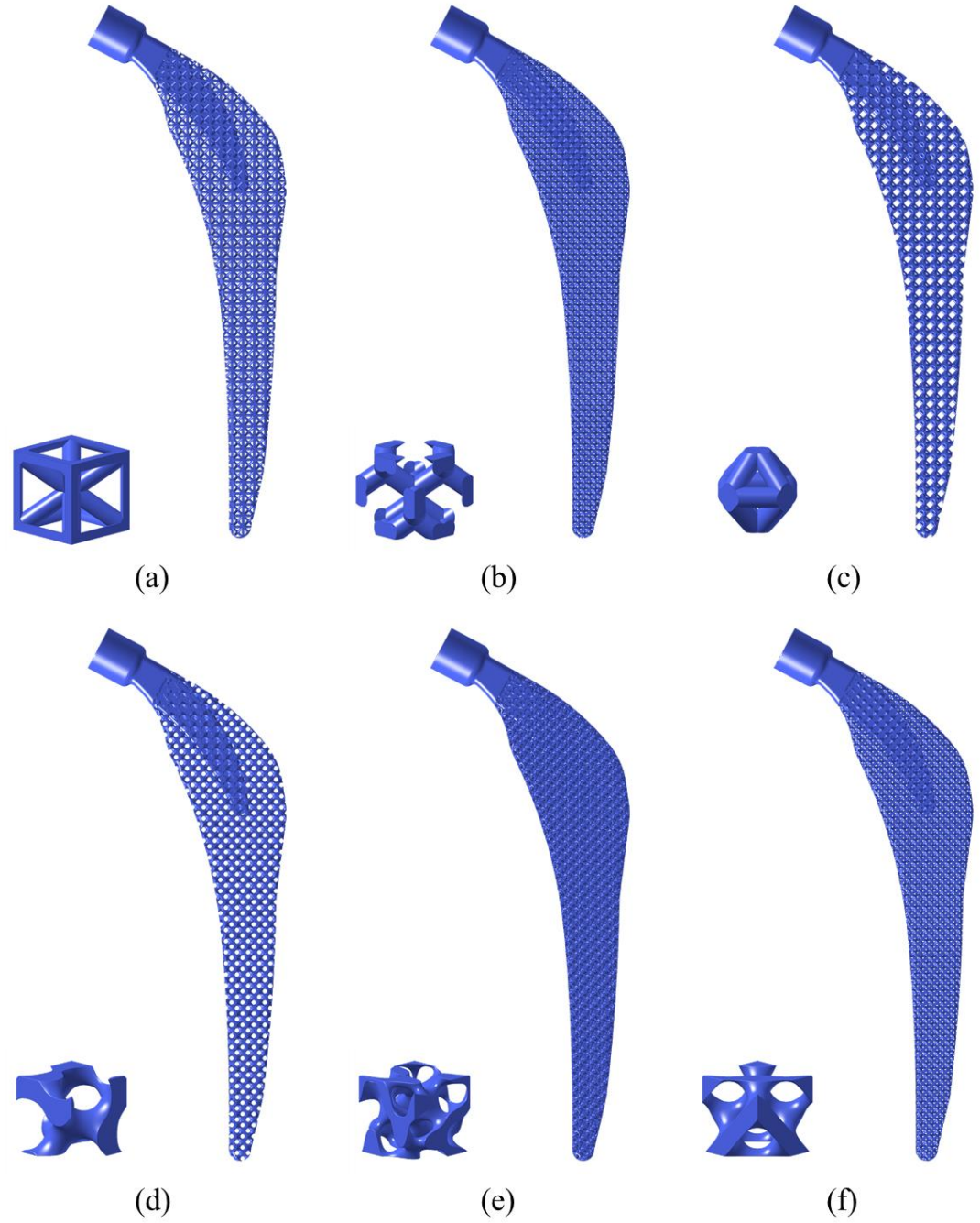

Fig. 3. 3D geometric models of endoprosthesis stem made of metamaterials based on following structures: (a) cubic with supports; (b) diamond; (c) double pyramid; (d) gyroid; (e) Fischer–Koch; (f) Schwarz D

Geometric model of test bench for endoprosthesis stem

A digital model of the virtual test bench intended for strength analysis of the femoral component of the hip endoprosthesis made from the selected metamaterials was developed following the procedure described in the GOST R ISO 7206-4-2012 standard

"Implants for surgery – Partial and total hip joint prostheses – Determination of endurance properties and performance of stemmed femoral components". This standard is aimed at strength predictions (including fatigue resistance under cyclic loads) of stemmed femoral components in total hip arthroplasty (THA), also used separately for partial hip prosthetics. The GOST standard is identical to the international standard ISO 7206-4:2010 "Implants for surgery — Partial and total hip joint prostheses — Part 4: Determination of endurance properties and performance of stemmed femoral components" [41]. According to the standard, the lower part of the test specimen is embedded into a solid medium; the head of the specimen is subjected to cyclic loading to produce axial compression, bending in two planes and torsion until failure occurs or the prescribed number of cycles are achieved.

Figure 4 shows the configuration of the medium-sized hip endoprosthesis stem (120–250 mm from the center of the femoral head to the most distal point of the stem) based on the GOST R ISO 7206-4-2012 standard. The implant is located in a cylindrical cup filled with solidifying bone cement at angles $\alpha = 10°$, $\beta = 9°$, determining the inclination of the stem axis in the frontal and sagittal planes. The height of the cup was not normalized; it was set to 120 mm in the digital model so as to preserve the key distance $D = 80$ mm from the center of the head to the level of stem fixation. The diameter of the cup was chosen equal to 60 mm to minimize the influence of rigid fixation of the cylinder surface formed.

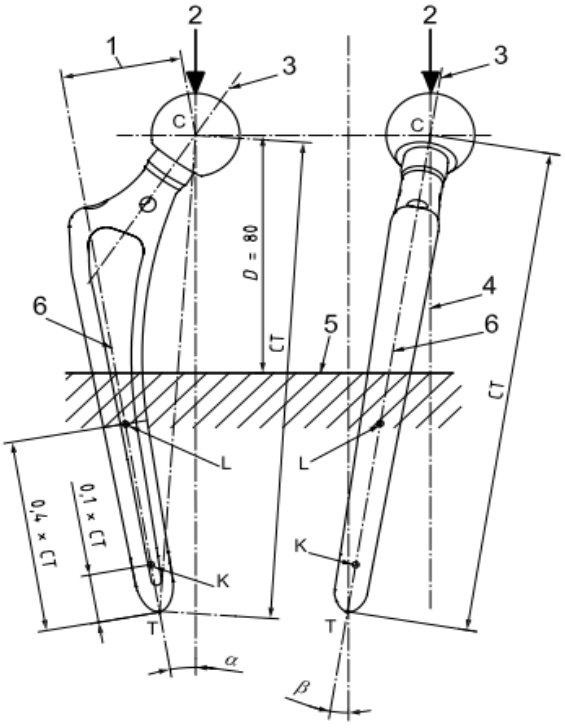

Fig. 4. Configuration of symmetrical endoprosthesis stems with CT distance of more than 120 mm, but less than or equal to 250 mm (based on GOST R ISO 7206-4-2012 (ISO 7206-4:2010)): arm *1* of head; load application point *2*; stem axis *3*; loading axis *4*; cement level *5*; stem axis KL *6*; T is the most distal point of the stem; C is the center of the head; D is the embedding level; K, L are points at certain distance from point T defining stem axis; α is the angle on the frontal plane CKL between loading axis *4* and stem axis *6*; β is the angle on sagittal plane perpendicular to CKL between loading axis *4* and stem axis *6*

The developed models of the metamaterial stem were combined in the Altair SimLab system with the constructed three-dimensional model of the cylinder made of bone cement using standard Boolean operations. The head of the femoral component was then added to the model as a truncated sphere.

This comprises a set of geometric models characterizing the biomechanical system, including the stem of the femoral component made from six types of metamaterials. A typical 3D numerical model of the implant–cement system is shown in Fig. 5.

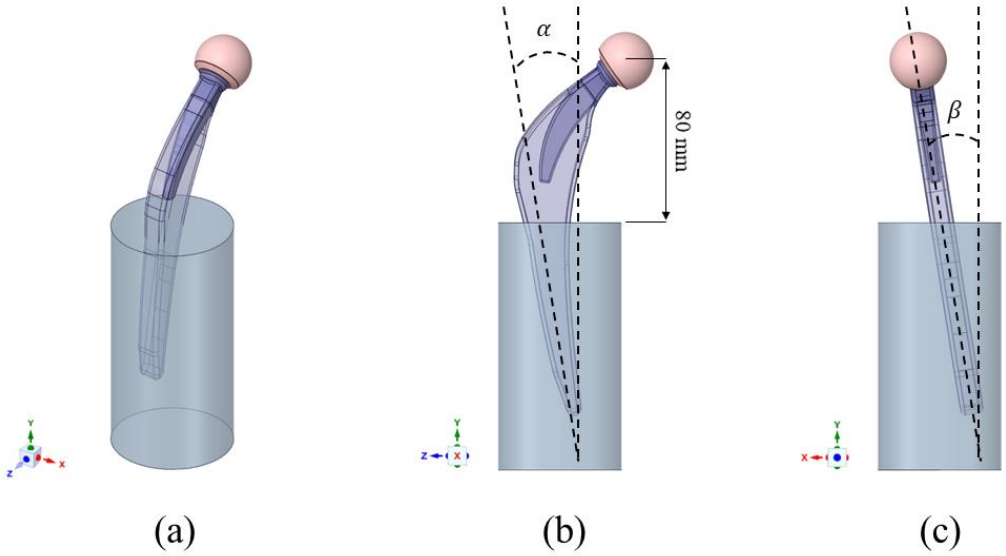

Fig. 5. Three-dimensional geometric model of implant–cement biomechanical system based on GOST R ISO 7206-4-2012 (ISO 7206-4:2010): (a) isometric view; (b) frontal view; (c) sagittal view

Finite element formulation for the problem on digital testing of the endoprosthesis stem

Three-dimensional geometric models of the virtual test bench (Fig. 5) were used to construct spatial finite element meshes with the tools of the Altair SimLab system. The developed numerical models are composed of tetrahedral finite elements with first-order displacement interpolation. The characteristic length of finite elements in the constructed mesh amounted to 0.2 mm for the stem, and to 1 mm for the ceramic head of the femoral component and the bone cement cylinder.

Finite element meshes characterizing the individual components of the system are constructed to have common nodes on adjacent surfaces of the components, with the exception of the interface between the implant and the ceramic head. The stem is rigidly fixed in bone cement in this approach, assuming no-slip, which is appropriate for both the given experimental setup following the standard guidelines and the developed porous structure of the metamaterial stem. From a computational standpoint, it is unnecessary to specify the contact interaction at the interfaces in this formulation (with the exception of the interface between the implant and the ceramic head, where the contact interaction is introduced into the model), yielding a faster and more stable solution.

The three-dimensional problem of elasticity theory describing the problem posed in the study is solved by the classical displacement-based finite element method using

the variational principle of minimum potential energy or generalization of the weighted residual method to three-dimensional problems [42].

The model (Fig. 5) is saved in INP format and exported to the Abaqus FEA suite to complete the finite element model and perform calculations of the stress-strain state for the fixed femoral component of the hip endoprosthesis as a system of solid deformable bodies. The formulation of the elasticity problem imposes the elastic properties of the materials used to manufacture the elements of the biomechanical system considered, the kinematic constraints and the acting forces.

According to the GOST R ISO 7206-4-2012 standard, a vertical load that is a total force of 2300 N is applied to the head of the femoral component (Fig. 4). Such a load is simulated in the finite element model by a concentrated force applied at a separate point (called Reference Point), mathematically connected to all nodes of the finite element mesh of the femoral head, ensuring a more uniform load distribution over the surface of the head (Fig. 6).

The kinematic constraints imposed assume that the outer surface of the cylinder is rigidly fixed, that is, all displacement components in the nodes of the finite element mesh on the outer surface are equal to zero (Fig. 6).

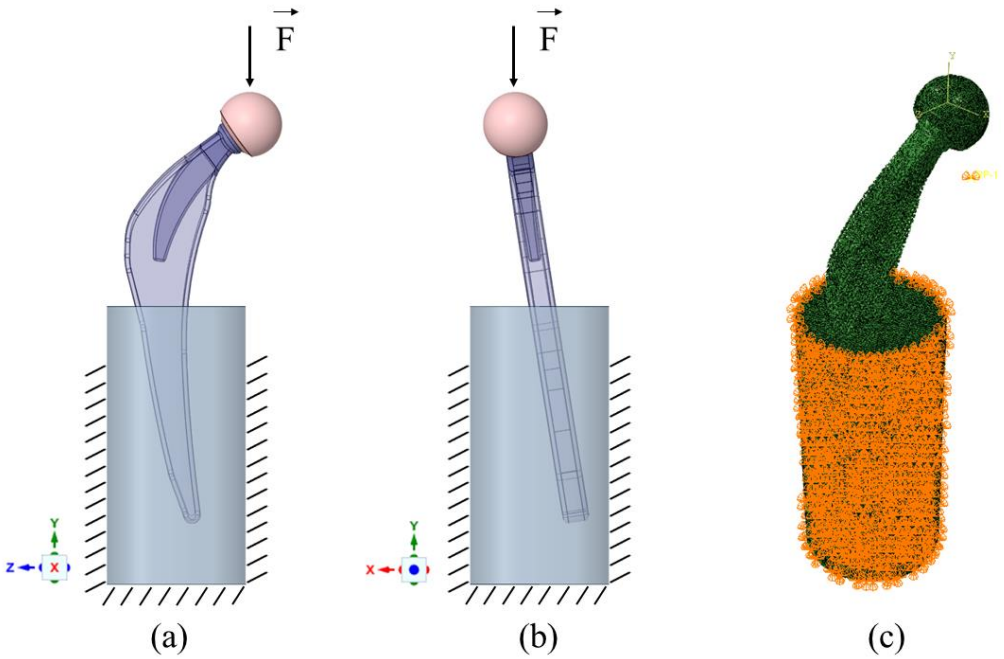

Fig. 6. Loading conditions for femoral component: (a) frontal view; (b)sagittal view; (c) isometric view of finite element model in Abaqus system

Setting the physical and mechanical properties of materials correctly is an extremely important factor for construction of high-fidelity digital models of virtual test environments. As mentioned above, the metamaterials in this paper are to be additively manufactured from the Ti_6Al_4V titanium alloy. The following parameter values were adopted for the mechanical properties of additive Ti_6Al_4V: density of 4.43 kg/m^3, Young's modulus of 113.8 GPa, Poisson's ratio of 0.342, yield strength of 950 MPa [43]. The fatigue properties of materials vary in a much wider range if different additive technologies and

subsequent surface treatments are introduced [44]. Analyzing the literature, we adopted a representative value of the fatigue limit equal to 350 MPa for the calculations with a symmetric loading cycle and a frequency of 10 Hz for Ti_6Al_4V titanium alloy obtained by the selective laser melting (SLM) technology [45,46].

The following mechanical characteristics were taken for the remaining components of the model: acrylic bone cement had a Young's modulus of 3.5 GPa, a Poisson's ratio of 0.3; the ceramic material of the femoral head had a Young's modulus of 0.43 GPa, a Poisson's ratio of 0.3 [47].

According to the GOST R ISO 7206-4-2012 standard, physical tests are aimed at evaluating the fatigue resistance of the endoprosthesis stem at a number of loading cycles set equal to $5 \cdot 10^6$. The system for inducing a quasi-static force to act on the head of the femoral component described in the standard functions with a pulsating loading cycle with a maximum force of 2300 N.

We determined the elastic displacements of the endoprosthesis stem, induced by the action of an applied force, and the integral stiffness of the structure with respect to the vertical displacements. Evaluating stiffness as a function of vertical displacements is of foremost interest, as it can provide deeper insights into the biomechanical behavior of the endoprosthesis The stiffness is calculated as follows: $k = \frac{F}{|U_2^{max}|}$, where is the k is the calculated stiffness of the endoprosthesis stem along the vertical direction; F is the magnitude of the vertical load; U_2^{max} is the maximum absolute value of the vertical component of the elastic displacement vector in the endoprosthesis stem.

Such a process was organized as follows for mathematical modeling of high-cycle fatigue strength using numerical analysis software:

1. Static elastic calculations of the stress–strain state of the biomechanical system under applied load (a force of 2300 N in our case) are carried out in Abaqus FEA software.
2. Computational results of the stress–strain state analysis, that is, the nodal values of displacements and components of the stress tensor, are exported to the Altair HyperLife system. Evaluation of the number of load cycles that the structure can withstand is then carried out based on the Wöhler curve set for the material used (in this case, Ti_6Al_4V titanium alloy) and the stresses in Gaussian nodes of finite elements.

The technique used in this study for evaluation of fatigue strength is incorporated in the Altair HyperLife software, using a well-known model for fatigue behavior of a material in the elastic range with a large number of symmetric loading cycles N_f, set by an exponential law within the range $N_1 < N_f < N_0$:

$$\sigma_a = S_f \left(N_f\right)^b, \tag{1}$$

where σ_a is the stress amplitude in a symmetric cycle , which the material can withstand at a given number of loading cycles N_f, S_f is the fatigue limit; b is the fatigue exponent calculated from the slope of the curve defined by Eq. (1) in logarithmic coordinates.

The parameters in Eq. (1) lie in the following ranges for common structural materials: $N_1 = 10^3$–10^4, $N_0 = 10^6$–10^7. It is assumed that the reference S–N curve for the fatigue limit of the material at point N_0, described by Eq. (1), has an inflection, after which the failure process either slows down or stops. In the latter case, the curve is

believed to extend to a horizontal section with a characteristic ordinate taken as the fatigue limit of the material under symmetric cyclic loading.

This model follows from the formulation of the problem on evaluating the fatigue limit of the endoprosthesis stem under a significant number of loading cycles beyond the inflection point on the $S–N$ curve. Evaluating the fatigue parameters of the Ti_6Al_4V titanium alloy by Eq. (1) with the fatigue limit of 350 MPa at $N_0 = 1{\cdot}10^6$ and the ultimate tensile strength of 1230 MPa, conditionally corresponding to $N_1 = 10^3$, we obtain the values of the fatigue limit equal to $S_f = 4323$ MPa and the exponent equal to $b = -0.182$. Evaluating the fatigue parameters of the Ti_6Al_4V titanium alloy by Eq. (1) with the fatigue limit of 350 MPa at $N_0 = 1{\cdot}10^6$ and the ultimate tensile strength of 1233 MPa, conditionally corresponding to $N_1 = 1$, we obtain the values of the fatigue limit equal to $S_f = 1233$ MPa and the exponent equal to $b = -0.092$.

The influence of the constant component of the cyclic load in an asymmetric loading cycle is determined by the ratio between the mean value and the amplitude of the stress cycle that the material can withstand at a given number of loading cycles [48]:

$$\frac{\sigma_a}{\sigma_{-1}} + \frac{\sigma_m}{\sigma_в} = 1, \quad (2)$$

where σ_a and σ_m are the amplitude and mean stress in an asymmetric loading cycle that the material can withstand at a given number of loading cycles N_f; σ_{-1} is the fatigue limit of the material during a symmetric loading cycle; $\sigma_в$ is the ultimate tensile strength of the material.

It follows from Eq. (2) that a linear decrease in the amplitude of the sustained stress cycle is observed with an increase in the constant component in the case of asymmetric loading:

$$\sigma_a = \sigma_{-1} - \varphi_\sigma \sigma_m, \text{ where } \varphi_\sigma = \frac{\sigma_{-1}}{\sigma_в} \quad (3)$$

Since the Wöhler curve is generally determined experimentally by uniaxial tensile testing, the stress tensor in the case of multiaxial yet in-phase loading is reduced to an equivalent nominal voltage at each point of the given structure and is used as the calculated parameter in Eq. (1). The maximum principal stress is taken as such nominal stress for brittle materials, and the von Mises equivalent stress with the sign corresponding to the sign of the maximum principal stress is taken for viscous materials.

The criterion for the critical state adopted in the fatigue calculations was the fatigue life, that is, the number of sustained cycles compared to the target value, selected as $5{\cdot}10^6$ cycles following the problem statement formulated in accordance with GOST R ISO 7206-4-2012. The Palmgren–Miner rule for damage accumulation was used for this purpose in the general case of a set of load scenarios, where failure occurs if the following inequality is satisfied:

$$\sum D_i = \sum \frac{n_i}{N_{if}} \geq 1.0\ , \quad (4)$$

where D_i is the damage during n_i cycles with load i; n_i is the number of stress cycles under load i ; N_{if} is the number of cycles to failure, taken from the $S–N$ curve for the combination of stress amplitude and mean stress level i.

Therefore, the stress values calculated in the finite elements at a given static load simulating a pulsating loading cycle can be used to evaluate the number of cycles that the structure can withstand at the selected points of the material from Eqs. (1) and (3), and determine the degree of damage to the structure from Eq. (4).

Results and Discussion

Effective properties of metamaterials

The effective elastic moduli of the metamaterials are necessary for comparing their integral characteristics, even though the moduli are not directly related to the structures made from these materials. In addition, their analysis is valuable from a biomechanical standpoint, since the stiffness of the endoprosthesis stem directly affects the processes of bone resorption in the contact area with metal. Importantly, regeneration of tissue also occurs in the pore space of the metamaterial, which is necessary for reliable cementless fixation of the femoral component in the medullary canal of long tubular bones of the human skeleton.

A detailed description of the homogenization procedures applied to these types of metamaterials is presented in our earlier studies [20,21]. The effective elastic moduli found for the metamaterials based on the titanium alloy are given in Table 1.

Table 1. Effective elastic moduli for six types of metamaterials (MPa)

Elastic constants	Cubic w. supports	Diamond	Double pyramid	Gyroid	Fischer–Koch	Schwarz D
E_1, MPa	8850.8	6251.3	10237.0	8423.0	10997.7	8795.7
E_2, MPa	8850.7	6251.2	10237.0	8402.3	11002.4	8795.7
E_3, MPa	8850.6	6251.0	10237.0	8413.1	10996.2	8797.2
G_{12}, MPa	4557.9	5234.6	4632.6	5036.9	5107.8	6325.5
G_{23}, MPa	4557.9	5234.6	4632.6	5035.9	5107.6	6327.2
G_{31}, MPa	4557.9	5234.6	4632.6	5037.5	5107.3	6326.5
ν_{12}	0.301	0.364	0.275	0.338	0.321	0.343
ν_{13}	0.301	0.364	0.275	0.337	0.321	0.343
ν_{23}	0.301	0.364	0.275	0.337	0.321	0.343

As seen from Table 1, the metamaterials are symmetric with respect to 90-degree rotation around any axis of the Cartesian coordinate system coinciding with the principal axes of geometric symmetry. However, despite the same values of effective elastic constants along the principal axes and in the principal planes, the homogenized models of these metamaterials as continuous media are not isotropic. This is easily verified by calculating Poisson's ratio using the well-known formula for isotropic continuum: $\nu = \frac{E}{2G} - 1$. The values obtained by this formula, -0.03; -0.4; 0.1; -0.16; 0.076; -0.3, differ significantly from those in Table 1, which confirms the anisotropic nature of the governing equations of metamaterials, despite apparent full symmetry.

Notably, high porosity leads to a significant decrease in stiffness along the principal axes of material symmetry compared to a solid material. For example, Young's modulus of the lattice structures lies in the range of 6.25–10.2 GPa, while that of the surface structures lies in the range of 8.4–11.0 GPa. The shear modulus of lattice metamaterials

lies in the range of 4.56–5.23 GPa, and that of surface metamaterials lies in the range of 5.04–6.33 GPa. Double pyramid and Fischer–Koch cells exhibit the highest Young's moduli with moderate shear moduli.

According to experimental studies of the proximal femur [49], Young's moduli of compact tissue lie in the range of 7500–17500 MPa in the longitudinal direction and 4000–7000 MPa in the transversal direction, depending on the density of the tissue. Thus, the values obtained for Young's moduli of the meta-biomaterials at a porosity of 70 % are closer to the lower bound for elastic moduli in compact tissue in the longitudinal direction, but slightly higher than their values in the transversal direction. From a biomechanical standpoint, such a range of elastic properties of meta-biomaterials can allow the compact femoral tissue to accommodate the load sufficiently so that bone resorption does not occur due to reduced stress level near the metal implant.

On the other hand, from a mechanobiological standpoint, the through-porosity of the metamaterial implant ensures penetration of biological fluid and bone matter in both radial and axial direction of the medullary canal, which is impossible in an endoprosthesis made of solid material. The high through-porosity of the metamaterial used to manufacture the endoprosthesis allows filling the internal volume of the metamaterial with a large amount of bioactive substance with mesenchymal stem cells and growth factors at the stage of surgery, with subsequent free penetration of active progenitor cells into the implant. This can improve reparative regeneration in the volume of meta-biomaterial, ultimately ensuring reliable osseointegration of the implant [9,50].

Analysis of elastic displacements and stiffness

Elastic displacements induced by the applied load integrally characterize the stiffness of the structure, which is an important factor in the stability of the endoprosthesis in the medullary canal during operation. According to the GOST R ISO 7206-4-2012 standard, physical tests are carried out in such a way that the permissible deviation of the test specimen from the vertical axis does not exceed 0.2 mm. Thus, we analyzed both vertical displacements characterizing the bending and stiffness of the stem, and horizontal displacements characterizing the deviation of the stem from the vertical position, which is a requirement of the GOST standard.

Figure 7 shows the fields of components and magnitude for the vector of elastic displacements, induced by the applied vertical force of 2300 N, for the considered types of meta-biomaterials.

As evident from the displacement fields in Fig. 7, the picture of the displacement distribution is similar for different types of metamaterial, regardless of the topology class (lattice or surface). The upper point of the endoprosthesis stem, located on the cylindrical structural element of the stem, securing the head of the femoral component, exhibits the largest displacements. We can evaluate the integral stiffness of the structure by analyzing the maximum displacements of the endoprosthesis head under the action of the applied load. All components and the magnitude of the displacement vector of the upper point, as well as the stiffness of the endoprosthesis stem, are given in Table 2.

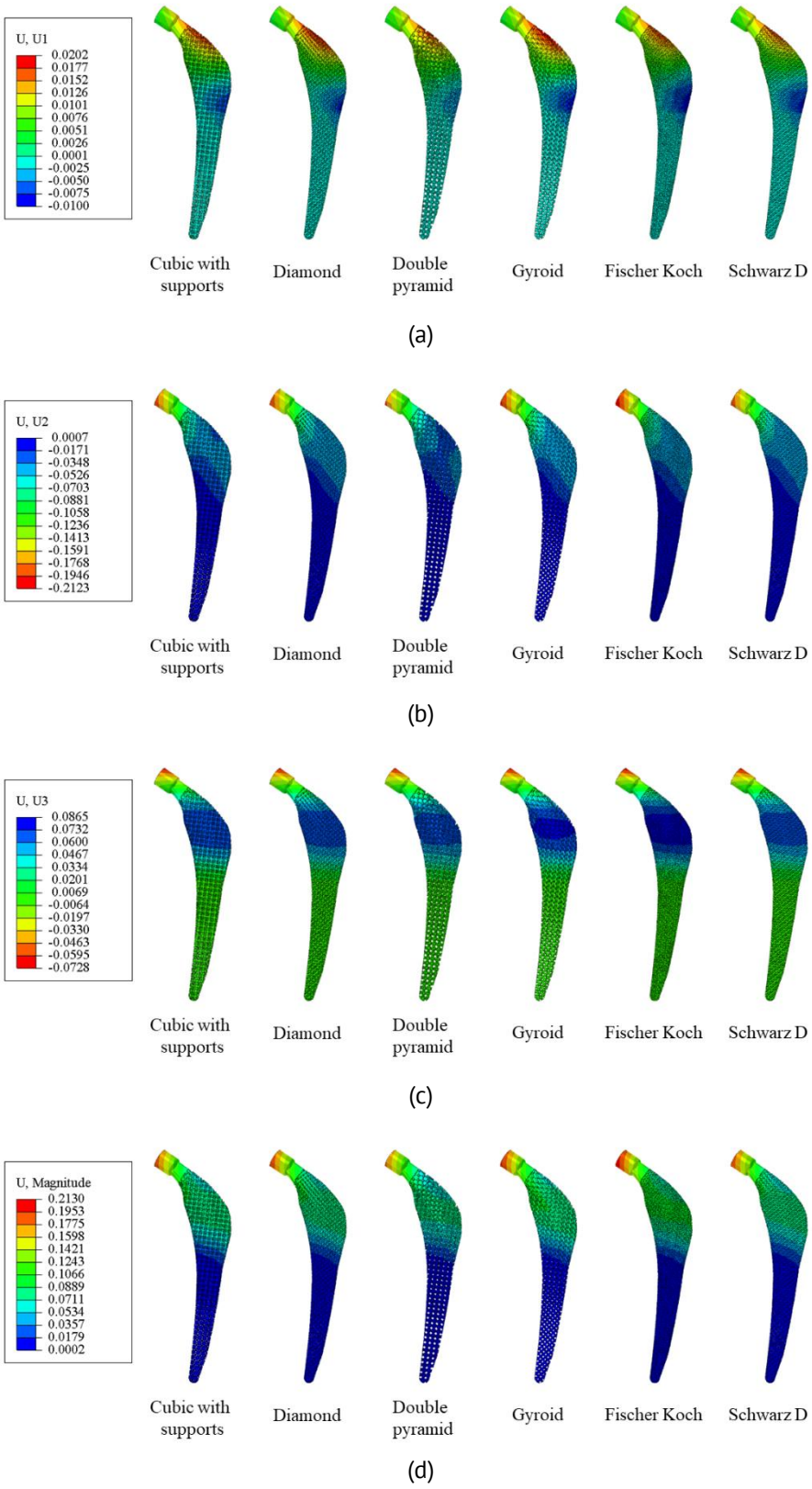

Fig. 7. Elastic displacement fields (in mm) in implant stem prepared from considered types of meta-biomaterial in the global coordinate system: (a) component along the X axis, in the median-sagittal plane; (b) component along the Y axis, in the vertical direction; (c) component along the Z axis, in the frontal plane; (d) displacement vector magnitude

Table 2. Displacements and stiffnesses for each type of implant stem

	Type of metamaterial cell					
	Cubic w. supports	**Diamond**	**Double pyramid**	**Gyroid**	**Fischer–Koch**	**Schwarz D**
U_1^{min}, mm	-0.008	-0.010	-0.006	-0.009	-0.010	-0.009
U_1^{max}, mm	0.019	0.020	0.017	0.020	0.018	0.018
U_2^{min}, mm	-0.0002	0.0003	-0.0003	-0.0003	0.0007	-0.0002
U_2^{max}, mm	-0.195	-0.198	-0.185	-0.203	-0.212	-0.195
U_3^{min}, mm	-0.071	-0.070	-0.069	-0.071	-0.073	-0.071
U_3^{max}, mm	0.074	0.073	0.069	0.080	0.087	0.072
U^{max}, mm	0.196	0.199	0.186	0.203	0.213	0.196
Stiffness, N/mm	11795	11616	12432	11330	10849	11795

The greatest contribution to the total displacement vector is expected to be made by the vertical component characterizing the elastic bending of the stem as a cantilever beam, fixed in the lower part and subjected to a bending moment at the end. The total displacements of the endoprosthesis head repeat the vertical displacements of the head with an accuracy to three significant digits. The maximum vertical displacement does not exceed 0.2 mm for such implants as Cubic w. supports, Diamond, Double pyramid and Schwarz D. The values of vertical displacements for the remaining implants, i.e., Gyroid and Fischer–Koch, are slightly higher than for the other implants, but by no more than 6 %.

Interestingly, small displacements are observed in the (XZ) plane of the middle part of the stem in the contact area between metal and bone cement. However, we believe that these displacements characterize the stiffness of the bone cement rather than the actual structure of the endoprosthesis stem and therefore are not of particular interest for this study. Nevertheless, it can be concluded that the endoprosthesis stem deviates from the vertical by less than 0.1 mm for all types of metamaterials, which is significantly less than the requirements in the GOST standard.

Multi-lattice structures designed to alleviate stress shielding were discussed in [51], with the weight of the implant reduced to 25 %. The elastic moduli of the lattice material cells varied in the range from 20 to 63 GPa with a porosity of 26–58%. The displacements of the model with the lattice structure exceed the displacements of the solid implant (4.04 and 3.81 mm, respectively), which is significantly higher than the displacements obtained in our study. Note that the model in [51] consisted of a femur with an implanted stem, and the load corresponded to a person with the weight of 700 N, walking at a normal speed, which could be the reason for the discrepancies with the results in our study.

An important mechanical factor affecting the biophysical processes in osteosynthesis with porous implants is the stiffness of the structure, which in the case of metamaterials is directly related to the internal structure, that is, the type and porosity of the unit cell. It was established in previous studies that the stiffness of the scaffold significantly affects the efficiency of the regeneration process in the pore space of the implant [9,15]. In particular, mathematical modeling of tissue regeneration in the scaffold volume with the porosity of 50 and 90 % [10,50] confirmed extensive osseointegration at lower amplitudes of the harmonic load in the case of greater porosity, which may be due a more pronounced effect of the mechanical stimulus deeper into the implant.

The stiffness of the metamaterial stem with a porosity of 70 %, calculated from vertical displacements, lies in the range of 11616–12432 N/mm for lattice structures and 10849–11795 N/mm for surface structures. Thus, lattice implants turn out to be stiffer than surface implants, which is extremely important from a mechanobiological standpoint. The stiffest metamaterial is the lattice type based on Double pyramid cell, and the least stiff is the surface type based on Fischer Koch cell, with the difference in stiffness amounting to almost 15 %, which is significant from a biomechanical standpoint.

A comparative analysis of experimental and computational data obtained in tests of the femoral component stem of the hip endoprosthesis following the ISO 7206-4:2010 requirements is presented in [32]. The bending stiffness was calculated for solid titanium and for a material with a random distribution of pore channels and an integral porosity of 33%, exhibiting a decrease by 47 % compared with the solid material in experimental measurements. The results were in good agreement with the full-scale test and the computational experiment for the solid implant and large discrepancies for the porous stem. However, despite the lower porosity, the stiffness of the porous endoprosthesis in [32] was only 1500 N/mm, which is significantly less than the stiffnesses obtained in our study. While there are some differences in the design of the stem at the macroscale, the main contribution to these discrepancies is probably made by the structure of the metamaterial compared to random porosity.

Stress and fatigue analysis

Analysis of the distribution of von Mises equivalent stresses indicates that the overall load on the implant is low (Fig. 8).

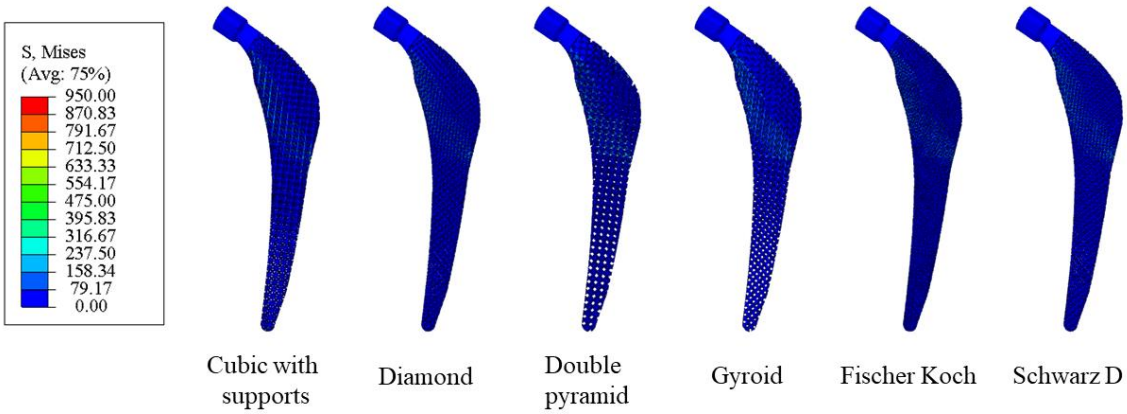

Fig. 8. Von Mises stress intensity (in MPa) in implant stems for each type of metamaterial

However, certain types of implants contain elements whose stress exceeds the yield strength of Ti_6Al_4V at 950 MPa. The maximum stresses are reached by thin elements appearing in the implant geometry due to its complex shape. As the unit cell does not fully fit into the endoprosthesis stem at its edge, there are regions where the strut comprising the metamaterial cell becomes geometrically thin and consequently capable of withstanding substantially lower loads. In view of this, the peak stress values are not a reliable indicator for assessing the applicability of the metamaterial in problems of this kind.

The stress distribution in the Diamond-type implant (Fig. 9) shows the most loaded zones, located along the lower (inner) edge of the stem and concentrated near the horizontal surface of bone cement.

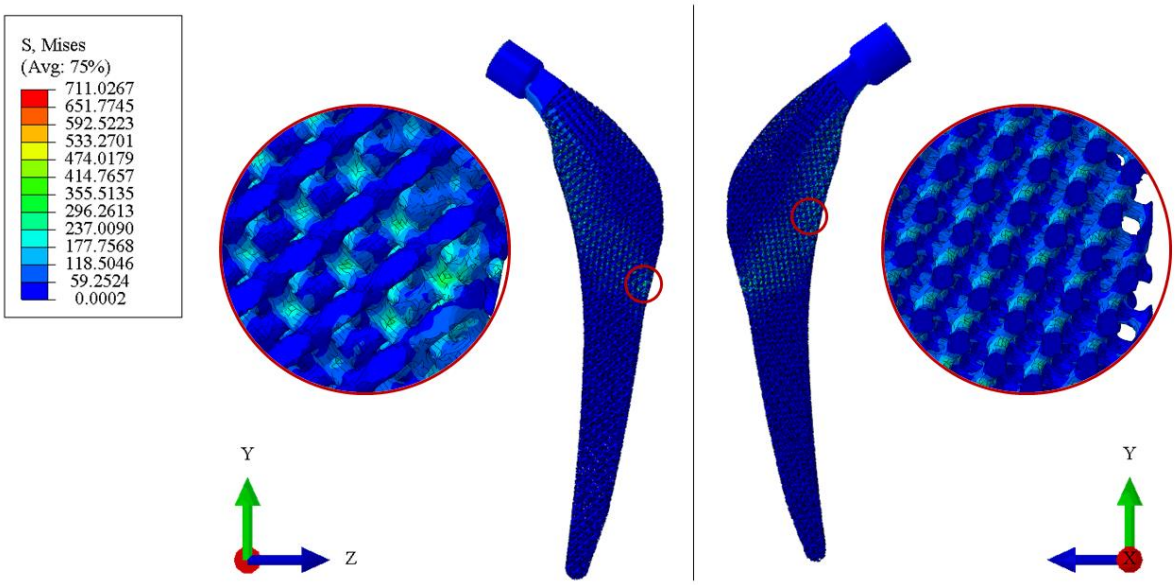

Fig. 9. Von Mises stress intensity (in MPa) in implant stem made of Diamond-type metamaterial

More detailed analysis of the stress state of the implant in each case can be carried out based on the histograms for the lattice (Fig. 10) and surface (Fig. 11) type metamaterials. The vertical axis characterizes the percentage of the implant volume located in the stress range plotted along the horizontal axis. More than 80 % of the implant volume for each type of metamaterial is in the stress range from 0 to 50, which does not exceed 5.3 % of the yield strength. More than 99 % of the volume does not exceed the fatigue limit of titanium alloy equal to 350 MPa. On average, implants made of lattice-type metamaterials have fewer stress concentrators, while Diamond and Double pyramid types do not exhibit regions where the yield strength of the titanium alloy is exceeded.

A small percentage of the implant volume is in the stress range exceeding the fatigue limit of 350 MPa. The number of elements reaching elevated stress values can be significantly reduced by refining the finite element model. Thin elements extending to the edge of the endoprosthesis stem often become stress concentrators and can be removed because they have no load-bearing capacity.

The distribution of stresses in the stem at the macroscale corresponds to both qualitative analytical predictions of the model describing bending in a cantilever beam subjected to a concentrated moment at the end, and studies by other authors evaluating the strength of hip endoprosthesis stems made of novel materials [18,39] The highest stresses occur on the inner surface of the leg in the bending region, reaching about 450 MPa in the case of the lattice gradient structure made from additive titanium alloy VT6 with a maximum vertical load of 2800 N described in [39]. Although the conditions of the numerical experiment and the porosity value of the considered metamaterials

differ, it can be argued that the stress values we calculated for this region (400–500 MPa) correspond to those presented in [39]. In general, the higher stress level in our case is due to the thinner beam or surface elements forming the metamaterial unit cells. Interestingly, a decrease in von Mises stresses was detected in [51] when part of the solid implant material was replaced with a multi-lattice structure.

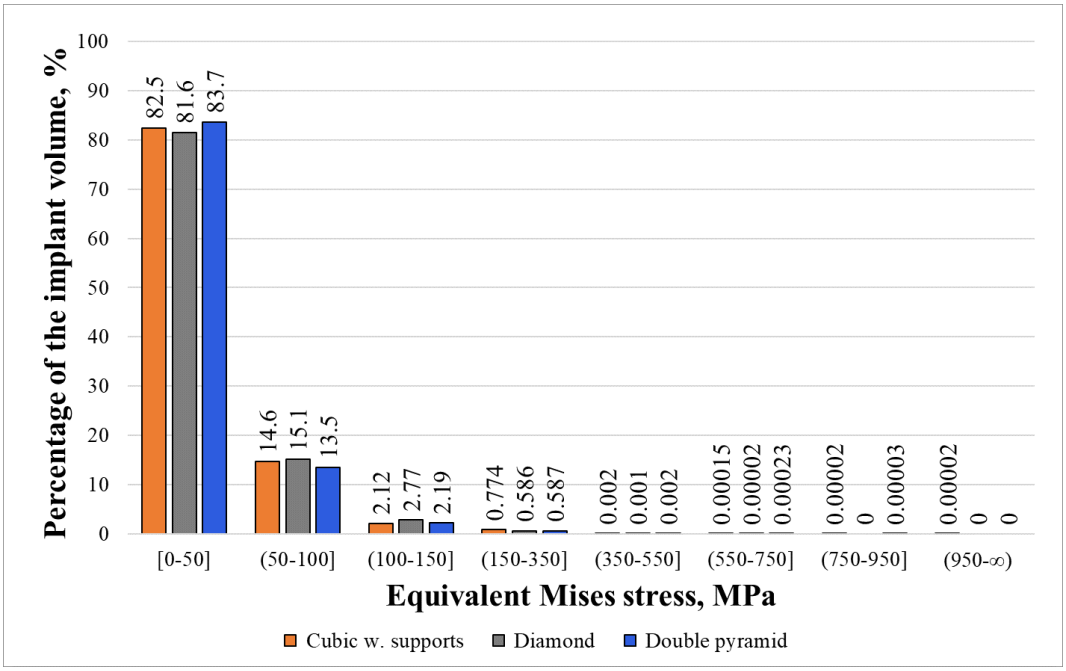

Fig. 10. Volume percentage in different stress ranges for implants based on lattice-type metamaterial

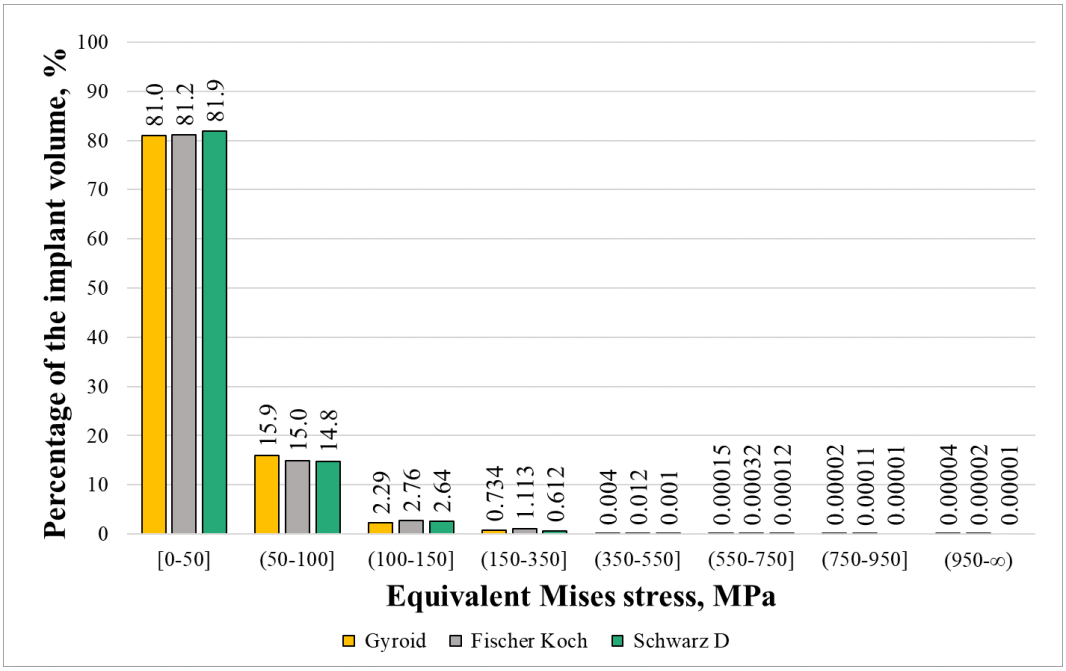

Fig. 11. Volume percentage in different stress ranges for implants based on surface-type metamaterial

Analysis of cyclic fatigue showed a general positive trend under high-cycle loading applied vertically to the surface of the implant head. The exception was a very insignificant fraction of the implant volume that could not withstand the number of cycles required by GOST (Table 3).

Table 3. Quantitative characteristics of fatigue in endoprosthesis stem

	Type of metamaterial cell					
	Cubic w. supports	**Diamond**	**Double pyramid**	**Gyroid**	**Fischer–Koch**	**Schwarz D**
Number of elements unable to withstand required number of cycles	27	1	32	39	40	32
Implant volume unable to withstand required number of cycles, %	$9.53 \cdot 10^{-5}$	$4.88 \cdot 10^{-6}$	$1.93 \cdot 10^{-4}$	$1.03 \cdot 10^{-4}$	$2.02 \cdot 10^{-4}$	$3.59 \cdot 10^{-5}$

Conclusion

Scaffolds and endoprostheses, that is, implants in a broad sense, manufactured from metamaterials are becoming increasingly widespread in tissue engineering and regenerative medicine, so it is of interest to determine the strength characteristics of such biomedical products. With this background in mind, we carried out a FEA-based theoretical study on the strength of a hip endoprosthesis stem manufactured entirely from highly porous meta-biomaterial, following the GOST R ISO 7206-4-2012 standard "Implants for surgery — Partial and total hip joint prostheses — Determination of endurance properties and performance of stemmed femoral components".

To design the endoprosthesis stem, we considered six configurations for the internal porous structure of the metamaterial based on biocompatible titanium alloy comprised by beam-type and TPMS unit cells. Digital 3D models of the hip endoprosthesis stem were constructed from elementary structural units. Evidently, the effective elastic moduli of the metamaterials lie in the range of physiological values of the cortical tissue in the femoral diaphysis, and the elastic moduli tensor has the property of material symmetry with respect to 90-degree rotation.

The standard procedure for testing the femoral components of endoprostheses was used to develop digital stands for simulating the loading process and calculate the stress–strain state of meta-biomaterial implants. The results obtained by finite element analysis of the structure prepared from various types of metamaterials generally confirm the load-bearing capacity of the given structures for the number of loading cycles set out by the standard.

We found potential issues that may arise if insufficient attention is paid to the complex shape of metamaterial implants and their additive manufacturing technology. In particular, replicating the smooth shape of the stem made of solid material with a lattice or surface meta-biomaterial can produce small regions of extremely low thickness, which

in turn leads to computational problems. Therefore, a direction we propose for future studies consists of developing new types of endoprostheses from meta-biomaterials, focusing closely on preserving the structure of the metamaterial near smooth surfaces with variable curvature.

We believe that digital tests can be used as a primary substitute for field experiments in developing new types of endoprostheses from meta-biomaterials.

References

1. Overvelde JT, Weaver JC, Hoberman C, Bertoldi K. Rational design of reconfigurable prismatic architected materials. *Nature*. 2017; 541: 347–352.
2. Bertoldi K, Vitelli V, Christensen J, van Hecke M. Flexible mechanical metamaterials. *Nature Reviews Materials*. 2017;2: 17066.
3. Watts CM, Liu X, Padilla WJ. Metamaterial electromagnetic wave absorbers. *Advanced Materials*. 2012;24: OP98–OP120.
4. Mei J, Ma G, Yang M, Yang Z, Wen W, Sheng P. Dark acoustic metamaterials as super absorbers for low-frequency sound. *Nature Communications*. 2012;3: 756.
5. Maslov LB. Study of vibrational characteristics of poroelastic mechanical systems. *Mechanics of Solids*. 2012;47(2): 221–233.
6. Zadpoor AA. Meta-biomaterials. *Biomaterials Science*. 2019;8(1): 18–38.
7. Cowin SC. (ed.) *Bone Mechanics Handbook*. 2nd ed. CRC Press; 2001.
8. van der Meulen MCH, Huiskes R. Why mechanobiology? A survey article. *Journal of Biomechanics*. 2002;35(4): 401–414.
9. Zadpoor AA. Bone tissue regeneration: the role of scaffold geometry. *Biomaterials Science*. 2015;3(2): 231–245.
10. Maslov LB. Biomechanical model and numerical analysis of tissue regeneration within a porous scaffold. *Mechanics of Solids*. 2020;55(7): 1115–1134.
11. Tonndorf R, Aibibu D, Cherif C. Isotropic and anisotropic scaffolds for tissue engineering: collagen, conventional, and textile fabrication technologies and properties. *Int. J. Mol. Sci*. 2021;22: 9561.
12. Hutmacher DW, Schantz J, Lam CX, Tan KC, Lim TC. State of the art and future directions of scaffold-based bone engineering from a biomaterials perspective. *J. Tissue Eng. Regen. Med*. 2007;1: 245–260.
13. Sumner DR, Turner TM, Igloria R, Urban RM, Galante JO. Functional adaptation and ingrowth of bone vary as a function of hip implant stiffness. *Journal of Biomechanics*. 1998:31; 909–917.
14. Wolff J. *Das Gesetz der Transformation der Knochen*. Berlin: A. Hirchwild; 1892.
15. Isaksson H. Recent advances in mechanobiological modeling of bone regeneration. *Mechanics Research Communications*. 2012;42: 22–31.
16. Ramakrishna S, Mayer J, Wintermantel E, Leong KW. Biomedical applications of polymer-composite materials: a review. *Composites Science and Technology*. 2001;61: 1189–1224.
17. Li CS, Vannabouathong C, Sprague S, Bhandari M. The use of carbon-fiber-reinforced (CFR) PEEK material in orthopedic implants: a systematic review. *Clin. Med. Insights Arthritis Musculoskelet. Disord*. 2015;8: 33–45.
18. Boudeau N, Liksonov D, Barriere T, Maslov L, Gelin JC. Composite based on polyetheretherketone reinforced with carbon fibres, an alternative to conventional materials for femoral implant: Manufacturing process and resulting structural behavior. *Materials & Design*. 2012;40(9): 148–156.
19. Maslov LB, Zhmaylo MA, Dmitryuk AYu, Kovalenko AN Study of the strength of a hip endoprosthesis made of polymeric material. *Russian Journal of Biomechanics*. 2022;4: 19-33.
20. Borovkov AI, Maslov LB, Zhmaylo MA, Tarasenko FD, Nezhinskaya LS. Elastic properties of additively produced metamaterials based on lattice structures. *Materials Physics and Mechanics*. 2023;51(7): 42-62.
21. Borovkov AI, Maslov LB, Zhmaylo MA, Tarasenko FD, Nezhinskaya LS. Finite element analysis of elastic properties of metamaterials based on triply periodic minimal surfaces. *Materials Physics and Mechanics*. 2024;52(2): 11–29.
22. Hanks B, Berthel J, Frecker M, Simpson TW. Mechanical properties of additively manufactured metal lattice structures: data review and design interface. *Addit. Manuf*. 2020;35: 101301.
23. Jia Z, Liu F, Jiang X, Wang L. Engineering lattice metamaterials for extreme property, programmability, and multifunctionality. *J. Appl. Phys*. 2020;127: 150901.

24. Feng J, Fu J, Lin Z, Shang C, Li B. A review of the design methods of complex topology structures for 3D printing. *Visual Computing for Industry, Biomedicine and Art.* 2018;1(1): 5.
25. Dong G, Tang Y, Zhao YF. A 149 line homogenization code for three-dimensional cellular materials written in MATLAB. *Journal of Engineering Materials and Technology.* 2019;141: 011005.
26. Bolshakov P, Raginov I, Egorov V, Kashapova R, Kashapov R, Baltina T, Sachenkov O. Design and optimization lattice endoprosthesis for long bones: Manufacturing and clinical experiment. *Materials.* 2020;13: 1185.
27. Bolshakov P, Kuchumov AG, Kharin N, Akifyev K, Statsenko E, Silberschmidt V. Method of computational design for additive manufacturing of hip endoprosthesis based on basic-cell concept. *Int. J. Numer. Meth. Biomed. Engng.* 2024;40(3): 3802.
28. Wieding J, Wolf A, Bader R. Numerical optimization of open-porous bone scaffold structures to match the elastic properties of human cortical bone. *J Mech Behav Biomed Mater.* 2014;37(9): 56-68.
29. Feng JW, Fu JZ, Yao XH, He Y. Triply periodic minimal surface (TPMS) porous structures: from multi-scale design, precise additive manufacturing to multidisciplinary applications. *Int. J. Extrem. Manuf.* 2022;4: 022001.
30. Gouveia RM, Koudouna E, Jester J, Figueiredo F, Connon CJ. Template curvature influences cell alignment to create improved human corneal tissue equivalents. *Adv. Biosyst.* 2017;1(12): 1700135.
31. Bobbert F, Zadpoor A. Effects of bone substitute architecture and surface properties on cell response, angiogenesis, and structure of new bone. *J. Mater. Chem. B.* 2017;5(31): 6175–6192.
32. Simoneau C, Terriault P, Jetté B, Dumas M, Brailovski V. Development of a porous metallic femoral stem: Design, manufacturing, simulation and mechanical testing. *Materials & Design.* 2017;114: 546–556.
33. Heinl P, Müller L, Körner C, Singer RF, Müller FA. Cellular Ti-6Al-4V structures with interconnected macro porosity for bone implants fabricated by selective electron beam melting. *Acta Biomater.* 2008;4: 1536–1544.
34. Parthasarathy J, Starly B, Raman S, Christensen A. Mechanical evaluation of porous titanium (Ti6Al4V) structures with electron beam melting (EBM). *J. Mech. Behav. Biomed. Mater.* 2010;3: 249–259.
35. Izri Z, Bijanzad A, Torabnia S, Lazoglu I. In silico evaluation of lattice designs for additively manufactured total hip implants. *Comput. Biol. Med.* 2022;144: 105353.
36. Shalimov AS, Tashkinov MA. Modeling of deformation and fracture of porous heterogeneous media taking into account their morphological composition. *PNRPU Mechanics Bulletin.* 2020;4: 175–187.
37. Zadpoor AA. Mechanical performance of additively manufactured meta-biomaterials. *Acta Biomater.* 2019;85: 41–59.
38. Tilton M, Lewis GS, Hast MW, Fox E, Manogharan G. Additively manufactured patient-specific prosthesis for tumor reconstruction: Design, process, and properties. *PLoS ONE.* 2021;16(7): e0253786.
39. Sufiiarov VSh, Orlov AV, Popovich AA, Chukovenkova MO, Soklakov AV, Mikhaluk DS. Numerical analysis of strength for an endoprosthesis made of a material with graded lattice structures. *Rus. J. Biomech.* 2021;25(1): 55–66.
40. Borovkov AI, Maslov LB, Zhmailo MA, Tarasenko FD, Nezhinskaya LS. Development of a gradient structure of the femoral component of a hip joint endoprosthesis based on a lattice-type metamaterial. In: *Collection of annotations of the 51st school-conference "Current problems of mechanics" in memory of D.A. Indianseva. Veliky Novgorod, June 19-21, 2024.* 2024. p.175–176. (In Russian)
41. International Standard. *ISO 7206-4:2010. Implants for surgery — Partial and total hip joint prostheses — Part 4: Determination of endurance properties and performance of stemmed femoral components (IDT).* OSO; 2010.
42. Maslov LB. *Finite element poroelastic models in biomechanics.* 2nd ed. St. Petersburg: Lan'; 2023. (In Russian)
43. Boyer R, Welsch G, Collings EW. *Materials properties handbook: titanium alloys*. ASM International; 1994.
44. Lewandowski JJ, Seifi M. Metal Additive Manufacturing: A Review of Mechanical Properties. *Annual Review of Materials Research.* 2016;46(1): 151–186.
45. Benedetti M, Cazzolli M, Fontanari V, Leoni M. Fatigue limit of Ti6Al4V alloy produced by Selective Laser Sintering. *Procedia Structural Integrity.* 2016;2: 3158–3167.
46. Günther J, Krewerth D, Lippmann T, Leuders S, Tröster T, Weidner A, Biermann H, Niendorf T. Fatigue life of additively manufactured Ti–6Al–4V in the very high cycle fatigue regime. *International Journal of Fatigue.* 2017;94: 236–245.
47. Kulmetyeva VB, Porozova SE. *Ceramic materials: production, properties, application.* Perm: Perm State Technical University Publishing House; 2009. (In Russian)
48. Birger IA, Mavlyutov RR. *Strength of materials*. Moscow: Nauka, 1986. (In Russian)
49. Wirtz DC, Schiffers N, Pandorf T, Radermacher K, Weichert D, Forst R. Critical evaluation of known bone material properties to realize anisotropic FE-simulation of the proximal femur. *J. Biomech.* 2000;33(10): 1325–1330.

50. Maslov LB. Mathematical model of bone regeneration in a porous implant. *Mechanics of Composite Materials.* 2017; 53(3): 399–414.
51. Gok MG. Creation and finite-element analysis of multi-lattice structure design in hip stem implant to reduce the stress-shielding effect. *Proceedings of the Institution of Mechanical Engineers, Part L: Journal of Materials: Design and Applications.* 2022;236(2): 429–439.

About Authors

Aleksey I. Borovkov
Candidate of Technical Sciences, Associate Professor
Vice-rector for digital transformation (Peter the Great St. Petersburg Polytechnic University, St. Petersburg, Russia)

Leonid B. Maslov
Doctor of Physical and Mathematical Sciences, Associate Professor
Lead Researcher (Peter the Great St. Petersburg Polytechnic University, St. Petersburg, Russia)
Lead Researcher (Ivanovo State Power Engineering University, Ivanovo, Russia)

Mikhail A. Zhmaylo
Master of Science
Lead Engineer (Peter the Great St. Petersburg Polytechnic University, St. Petersburg, Russia)

Fedor D. Tarasenko
Master of Science
Lead Engineer (Peter the Great St. Petersburg Polytechnic University, St. Petersburg, Russia)

Liliya S. Nezhinskaya
Bachelor of Science
Engineer (Peter the Great St. Petersburg Polytechnic University, St. Petersburg, Russia)